Piotr Zabielski,[1] Ian R. Lanza,[1] Srinivas Gopala,[1] Carrie J. Holtz Heppelmann,[2] H. Robert Bergen III,[2] Surendra Dasari,[3] and K. Sreekumaran Nair[1]

Altered Skeletal Muscle Mitochondrial Proteome As the Basis of Disruption of Mitochondrial Function in Diabetic Mice

Diabetes 2016;65:561–573 | DOI: 10.2337/db15-0823

Insulin plays pivotal role in cellular fuel metabolism in skeletal muscle. Despite being the primary site of energy metabolism, the underlying mechanism on how insulin deficiency deranges skeletal muscle mitochondrial physiology remains to be fully understood. Here we report an important link between altered skeletal muscle proteome homeostasis and mitochondrial physiology during insulin deficiency. Deprivation of insulin in streptozotocin-induced diabetic mice decreased mitochondrial ATP production, reduced coupling and phosphorylation efficiency, and increased oxidant emission in skeletal muscle. Proteomic survey revealed that the mitochondrial derangements during insulin deficiency were related to increased mitochondrial protein degradation and decreased protein synthesis, resulting in reduced abundance of proteins involved in mitochondrial respiration and β-oxidation. However, a paradoxical upregulation of proteins involved in cellular uptake of fatty acids triggered an accumulation of incomplete fatty acid oxidation products in skeletal muscle. These data implicate a mismatch of β-oxidation and fatty acid uptake as a mechanism leading to increased oxidative stress in diabetes. This notion was supported by elevated oxidative stress in cultured myotubes exposed to palmitate in the presence of a β-oxidation inhibitor. Together, these results indicate that insulin deficiency alters the balance of proteins involved in fatty acid transport and oxidation in skeletal muscle, leading to impaired mitochondrial function and increased oxidative stress.

Prior studies reported the key role of insulin in regulating mitochondrial biogenesis (1–3) and fuel metabolism (4). Insulin deficiency in humans with type 1 diabetes (T1D) reduces mitochondrial ATP production (5) despite elevated whole-body oxygen consumption (6,7), suggesting an uncoupled respiration. However, the molecular link between insulin levels, oxidative stress, and altered mitochondrial function remains unclear.

Mitochondrial function is determined by its proteome quantity and quality. Here we hypothesized that insulin deficiency alters mitochondrial proteome homeostasis (proteostasis) as a mechanistic explanation for altered mitochondrial physiology in diabetes. The rationale for this hypothesis is that insulin is a key hormone regulating muscle protein turnover (8–10), which is critical for maintaining not only protein concentrations but also protein quality and function. The effect of insulin on muscle protein synthesis varies considerably among different proteins (11). Insulin has been shown to stimulate muscle mitochondrial protein synthesis in swine (2) and when coinfused with amino acids in humans (3); yet, it does not affect synthesis of myosin heavy chain (12). These observations indicate that insulin selectively stimulates synthesis and expression of specific proteins with potential effect on mitochondrial function. Previous studies also demonstrated that ceramides and long-chain fatty acyl CoAs accumulate in muscle during insulin deficiency (13) and that oxidation of long-chain fatty acids (FAs)

[1]Division of Endocrinology, Diabetes, Metabolism, and Nutrition, Mayo Clinic College of Medicine, Rochester, MN
[2]Department of Biochemistry and Molecular Biology, Mayo Clinic College of Medicine, Rochester, MN
[3]Division of Biomedical Statistics and Informatics, Mayo Clinic College of Medicine, Rochester, MN
Corresponding author: K. Sreekumaran Nair, nair@mayo.edu.

Received 16 June 2015 and accepted 1 December 2015.

This article contains Supplementary Data online at http://diabetes.diabetesjournals.org/lookup/suppl/doi:10.2337/db15-0823/-/DC1.

P.Z. is currently affiliated with the Department of Physiology, Medical University of Bialystok, Bialystok, Poland. S.G. is currently affiliated with the Department of Biochemistry, Sree Chitra Tirunal Institute for Medical Sciences and Technology, Trivandrum, India.

© 2016 by the American Diabetes Association. Readers may use this article as long as the work is properly cited, the use is educational and not for profit, and the work is not altered.

increase reactive oxygen species (ROS) production (14). Moreover, the composition of plasma acyl-carnitines are altered in T1D (15,16) and type 2 diabetes (T2D) (17,18), likely consequent to defective β-oxidation.

A critical question is whether insulin deprivation affects the expression of individual mitochondrial proteins that may explain altered mitochondrial fuel metabolism. Proteome analyses in heart muscle found upregulation (19) or downregulation (20) of β-oxidation proteins in different diabetic models. How insulin deficiency affects the mitochondrial proteome in skeletal muscle and whether changes in its proteome homeostasis could explain the muscle mitochondrial changes seen in diabetes are currently unknown. Moreover, most of the previous studies involving heart proteome and mitochondrial studies were performed only in insulin-deficient states mostly immediately after inducing diabetes by streptozotocin (STZ), and most lack a clinically relevant insulin-treated group. Moreover, studying insulin deficiency effect in STZ-induced mice treated with insulin after a period of stabilization will allow delineation of STZ effect. Inclusion of insulin-treated animals could also shed light on the possible alternations still present in skeletal muscle of diabetic mice treated by insulin by a peripheral route. Such knowledge would provide important mechanistic insight into insulin deprivation and peripheral insulin treatment on skeletal muscle metabolism in both insulin-treated and -deprived T1D. We accomplished this goal by induction of diabetes by double high-dose injection of STZ and subsequent treatment of STZ-induced diabetic mice with subcutaneous insulin implants, which ensure long-lasting glycemic control, which is hard to achieve in mice with an injectable insulin regimen.

Here we comprehensively evaluated skeletal muscle mitochondrial physiology in insulin-deprived STZ-induced diabetic mice (STZ−I) compared with nondiabetic (ND) controls and insulin-treated STZ-induced diabetic mice (STZ+I). Although exogenous insulin treatment cannot normalize all diabetes complications in humans, we sought to determine if exogenous insulin could normalize mitochondrial function and protein expression in STZ mice. The use of stable isotope-based high-throughput proteomics and lipidomic analyses in skeletal muscle allowed us to gain mechanistic insight into the effects of insulin deprivation and treatment on skeletal muscle oxidative metabolism.

RESEARCH DESIGN AND METHODS

Animals

Male 13-week-old C57BL/6J mice (The Jackson Laboratory, Bar Harbor, ME) were acclimated for 1 week before the experiment in standard animal facility conditions. The protocol was approved by the Mayo Clinic Institutional Animal Care and Use Committee. Diabetes was induced by double high-dose intraperitoneal injection of STZ, as described previously (13), which generates animals without residual β-cell function. To exclude any adverse effects of acute STZ toxicity and other adverse factors, such as initial hypoglycemia and stress, we treated all diabetic animals with the subcutaneous LinBit insulin implant at 0.2 units/24 h, ~8 U/kg/day (LinShin Canada, Inc., Toronto, ON, Canada). ND animals received implants without insulin. The initial 3-week insulin treatment ensured that animals regained weight and were well past the toxic effect of STZ.

After 3 weeks of insulin therapy, diabetic insulin-treated animals were randomly divided into STZ−I and STZ+I groups. The insulin was discontinued in the STZ−I group by removing implants, which resulted in return of the diabetic phenotype. Mice were killed 1 week later, and the quadriceps muscle was harvested for mitochondrial and proteomic analysis. Before the mice were killed, body composition was measured by MRI (EchoMRI, Houston, TX) and energy expenditure and physical activity were measured over 24 h by a cage calorimetry system, as described previously (21). Plasma glucose, ketones, HbA_{1c}, and free FAs (FFAs) content were measured, as described earlier (18).

Mitochondrial Respiration

Mitochondrial respiration and coupling efficiency was measured by high-resolution respirometry in isolated quadriceps skeletal muscle mitochondria, as described earlier (22). Combinations included isolated mitochondria only (respiratory state 1), 10 mmol/L glutamate and 2 mmol/L malate (state 2), 2.5 mmol/L ADP (state 3, complex I [CI]), 10 mmol/L succinate (state 3, CI+CII), 0.5 μmol/L rotenone (state 3, CII), 2 μg/mL oligomycin (state 4), 2.5 μmol/L carbonyl cyanide p-trifluoromethoxyphenylhydrazone (FCCP; protonophoric respiration uncoupler), and 2.5 μmol/L antimycin A (electron transport chain inhibitor). Measurements were performed in duplicate and averaged. Oxygen flux rates were expressed per tissue wet weight and per milligram of mitochondrial protein as measured by Pierce 660-nm protein assay.

Mitochondrial ATP Synthesis

Mitochondrial ATP synthesis rates were measured by bioluminescence using a luciferin–luciferase reaction and Veritas Microplate luminometer (Turner BioSystems, Sunnyvale, CA), as described earlier (1). Substrate combinations included 10 mmol/L glutamate with 1 mmol/L malate, 20 mmol/L succinate with 0.1 mmol/L rotenone, 0.05 mmol/L palmitoyl-L-carnitine with 1 mmol/L malate, 1 mmol/L pyruvate with 0.05 mmol/L palmitoyl-L-carnitine, 10 mmol/L α-ketoglutarate, and 1 mmol/L malate.

Mitochondrial H_2O_2 Emission

Mitochondrial H_2O_2 production was measured by continuous monitoring of Amplex Red oxidation (Invitrogen Corp., Carlsbad, CA) using a Fluorolog 3 spectrofluorometer (Horiba Scientific, Kyoto, Japan), as described previously (22). Background fluorescence was measured in deenergized mitochondria (state 1 respiration), followed by stepwise addition of 10 mmol/L glutamate and 2 mmol/L malate (state 2, CI), 10 mmol/L succinate (state 2, CI+II), 2.5 mmol/L ADP (state 3 CI+II), 2 μg/mL oligomycin (state 4 CI+II), 0.5 μmol/L rotenone (state 4 CII), 2.5 μmol/L FCCP (uncoupled), and 2.5 μmol/L antimycin A (respiration inhibitor).

High-Throughput Differential Proteomic Analysis by Stable Isotope Labeling of Amino Acids in Cell Culture Mouse Approach

Quadriceps muscle tissue from fully labeled mice, generated by in vivo stable isotope labeling of amino acids (SILAC mice; $^{13}C_6$-L-lysine, >98% labeled in tissue proteins) was used as a reference standard to compare the relative expression of quadriceps muscle proteins in ND, STZ−I, and STZ+I mice (n = 6 per group) by mass spectrometry (MS), as described in the Supplementary Data. We used the Mascot protein identification engine and false discovery rate approach to identify peptides in MS spectra. Relative protein expression between experimental groups was measured using Rosetta Elucidator software weighted statistics. Vinculin was used as a loading control and revealed no significant differences in sample/SILAC mixing and SDS-PAGE sample loading (Supplementary Table 1). A detailed description of all of the identified and quantified proteins from ND, STZ–I, and STZ+I groups is contained in the Supplementary Data.

Pathway Analysis of Proteomics Data

Pathway enrichment analysis was performed using IPA software (Ingenuity Systems, Inc., Redwood City, CA), as described earlier (22). Multiple data entries of the same protein were resolved by IPA software by filtering entries by their lowest P value. Only proteins with $P < 0.05$ between groups were taken into consideration. To identify significantly affected pathways, the Fisher exact test was used, and P values were expressed as their $-\log_{10}$ derivatives (e.g., $P < 0.05$ corresponds to $P > 1.301$ on $-\log_{10}$ scale). In addition, we compared the resulting proteomic data set with the MitoCarta 2.0 mouse mitochondrial proteins database (23).

Semitryptic Peptides Detection and Quantification

We followed a two-step workflow to detect and quantify semitryptic peptides from MS/MS data of each mice cohort (n = 3 per group). The details of this approach have been previously reported (22).

Mixed Muscle Protein Synthesis Rates

The fractional synthesis rates of mixed muscle proteins were measured in mice quadriceps skeletal muscle using L-[ring-$^{13}C_6$]phenylalanine (Cambridge Isotope Laboratories, Tewksbury, MA) and MS, as described earlier (22,24,25).

Immunoblotting

Tissue was pulverized in LN_2 and homogenized by sonication on ice in radioimmunoprecipitation assay buffer (Sigma-Aldrich, St. Louis, MO). After denaturation in loading buffer, samples were separated by and blotted to nitrocellulose membranes. Membranes were blocked in TBS Odyssey Blocking Buffer (LI-COR, Lincoln, NE) before being incubated overnight with primary rabbit, anti-mouse antibodies for the proteins of interest. Proteins were detected by infrared fluorescent detection (LI-COR Odyssey) using appropriate anti-mouse and anti-rabbit secondary antibodies (LI-COR).

Tissue Acyl-Carnitine Profiling

Skeletal muscle concentration of 30 acyl-carnitine species were measured using deuterated internal standards and liquid chromatography/MS/MS, as described previously (26). Individual carnitine and acyl-carnitines were quantified against the nearest labeled internal standard and standard curves prepared on synthetic compounds. The carnitine palmitoyltransferase 1 (CPT1) activity index was measured by dividing free L-carnitine value by the sum of C16 and C18 acyl-carnitines (27). Short-chain and very long-chain acyl-CoA dehydrogenase indexes were calculated according to Chace et al. (26).

Cell Culture

Differentiated C2C12 myotubes were prepared as described by Boyle et al. (28). To mimic insulinemia, differentiation was done in serum-poor medium without additional insulin. The differentiated myotubes were incubated for 15 h with albumin-conjugated palmitic acid in differentiation medium. Control cells were incubated with an equal concentration of BSA and ethanol/DMSO. Methylene cyclopropyl acetic acid (MCPA; short- [SCAD] and medium-chain [MCAD] acyl-CoA dehydrogenase inhibitor) was added to a medium at the concentration of 500 μmol/L just before its addition to the cells.

Oxygraph Studies in C2C12 Cells

Mitochondrial respiration in permeabilized C2C12 cells was measured according to Boyle et al. (28). Myotubes treated according to the experimental conditions were harvested, resuspended in mitochondrial respiration buffer, permeabilized with digitonin, and immediately transferred to an Oroboros Oxygraph-2K respiration chamber (~1–1.5 × 10^6 cells/2 mL; Oroboros Instruments Corp., Innsbruck, Austria). Compounds were added sequentially to a final concentration indicated: state 1, myotubes; state 2, 5 μmol/L palmitoyl carnitine and 1 mmol/L malate; state 3 (CI), 2 mmol/L ADP, 10 μmol/L cytochrome C, and 2 mmol/L glutamate; state 3 (CI+CII), 3 mmol/L succinate; state 4 (CI+CII), 2.5 μg/L oligomycin; uncoupled (CI+CII), 2.5 μmol/L FCCP; uncoupled (CI), 0.5 μmol/L rotenone; and AA, 2.5 μmol/L antimycin A. Experiments for control, palmitate, palmitate+MCPA, and MCPA alone were done in triplicate samples.

ROS Production in C2C12 Cells

Intracellular conversion of nitro blue tetrazolium (Sigma-Aldrich) to formazan by superoxide anion was used to measure the generation of ROS in C2C12 myotubes, as previously described (29).

Statistical Analysis

Statistical significance among groups for all the measurements, except differential proteomics, was estimated using ANOVA with the Tukey honest significant difference post hoc test. Significance level was set to $P < 0.05$. Significant differences in individual protein expression from the proteomic data set were identified using the z-statistic, as described earlier (22).

RESULTS

Body Composition and Biochemical Parameters

STZ–I were smaller and leaner than ND controls or STZ+I (Supplementary Fig. 1*A*). Although STZ–I had lower total body water, their hydration ratio was similar to ND controls, showing that diabetic animals were not dehydrated (Supplementary Fig. 1*B* and *C*). As expected, plasma glucose, ketones, FFA, and HbA_{1c} were higher in STZ–I mice than in STZ+I and ND mice (Supplementary Fig. 1*D*–*G*). The respiratory quotient was lower in STZ–I compared with STZ+I or ND, indicating greater reliance on fat as a fuel substrate during insulin deprivation (Supplementary Fig. 1*H*–*J*). Total energy expenditure (Supplementary Fig. 1*K*) and physical activity (Supplementary Fig. 1*L*) were decreased in STZ–I and STZ+I, but the activity-normalized estimate of the resting metabolic rate was higher in STZ–I animals and restored in STZ+I (Supplementary Fig. 1*M*). These data indicate that insulin deprivation in STZ mice elicits whole-body metabolic changes characteristic of T1D (6,30), which were largely reversed with exogenous insulin treatment, similar to previous observations in diabetic dogs (31). Elevated HbA_{1c} in STZ+I mice (Supplementary Fig. 1*G*) is likely due to postprandial hyperglycemia (6:30 A.M. plasma glucose in STZ+I mice was 297 ± 28 mg/dL) that was not evident after 3 h of fasting before the experiment (Supplementary Fig. 1*D*).

Muscle Mitochondrial Dysfunction With Insulin Deprivation

Mitochondrial oxygen consumption and ATP production were measured in mitochondria isolated from quadriceps muscle. Maximal (state 3) and submaximal (states 1, 2, and 4) mitochondrial respiration were similar in all groups of mice (Fig. 1*A* and Supplementary Fig. 2*A*). In contrast, insulin deprivation decreased the levels of mitochondrial CI, CII, and CV, which, with the exception of CII, were restored by insulin treatment (Fig. 1*B*). Insulin deprivation lowered mitochondrial coupling efficiency. Decreased respiratory control ratios in STZ–I demonstrates greater mitochondrial proton leak (Fig. 1*C*) and reduction in phosphorylation efficiency (Fig. 1*D*). Consistent with the notion of mitochondrial uncoupling, mitochondrial ATP production rates were lower in STZ–I (Fig. 1*E* and Supplementary Fig. 2*B*). Uncoupled respiration is accompanied by greater mitochondrial ROS emissions as insulin deprivation markedly increased H_2O_2 emissions, which were attenuated, albeit incompletely, by insulin treatment (Fig. 1*F* and Supplementary Fig. 2*C*). Taken together, the parallel measurements of oxygen consumption and ROS production indicate that a greater percentage of mitochondrial O_2 consumption was accounted for by ROS production in STZ–I compared with ND or STZ+I (Fig. 1*G*). Interestingly, mitochondrial Mn superoxide dismutase (MnSOD) was decreased (Fig. 1*H*). As an additional marker of compromised cellular energy status, AMP-sensitive adenylate kinase 1 expression was elevated with insulin deprivation (Fig. 1*H*). Altogether, these results indicate that insulin deprivation disrupts mitochondrial function in the form of impaired mitochondrial ATP production, decreased phosphorylation efficiency, and greater ROS emission.

Insulin Deprivation Decreases Mitochondrial Protein Expression and Shifts the Balance of Cellular Lipid Transport Proteins

A SILAC mouse–assisted proteomic survey suggested that derangements in mitochondrial physiology could be explained by altered muscle proteome. A total of 149 proteins involved in energy metabolism were significantly altered in STZ–I mice compared with ND (Fig. 2*A* and Supplementary Table 2*A*). Consistent with the measurements of mitochondrial function, mitochondrial proteins of electron transport chain (ETC), tricarboxylic acid (TCA) cycle, and β-oxidation were downregulated in STZ–I compared with ND. Paradoxically, the proteins involved in myocellular uptake of FAs were upregulated. Proteins involved in muscular glycolysis and glycogen breakdown were upregulated, whereas those involved in pyruvate generation and mitochondrial transport were downregulated. Altogether, these proteomics data indicate clear patterns of upregulated glycolysis and glycogen breakdown during insulin deprivation, decreased mitochondrial respiratory chain proteins, and increased muscle uptake of lipids.

A comparison of STZ–I with STZ+I revealed 275 differentially expressed proteins, including 77 involved in energy metabolism (Fig. 2*B* and Supplementary Table 2*B*). Insulin treatment upregulated expression of proteins involved in β-oxidation and FA uptake but downregulated glycolysis and glycogen breakdown, thus upregulating carbohydrate storage. Thus, we provide proteomic evidence that insulin treatment restored the expression of proteins related to FA transport and glycolysis, but not all proteins involved in mitochondrial respiration were restored. Compared with ND mice, STZ+I animals still displayed downregulation of mitochondrial proteins involved in ETC/TCA and β-oxidation, with lesser difference in the expression of FA transport and glycolysis-related one (Fig. 2*C*, Supplementary Fig. 3, and Supplementary Table 2*C*). Overall, the data indicate that insulin deprivation markedly reduced the abundance of mitochondrial proteins involved in energy metabolism, including lipid oxidation, yet increased the abundance of proteins involved in cellular FA uptake. Although insulin treatment did not completely normalize the expression of mitochondrial proteins, there was a clear reversal of the FA transporters and glycolysis/glycogen breakdown proteins.

Proteomic Evidence of Oxidative Stress, Decreased Protein Synthesis, and Increased Protein Degradation With Insulin Deprivation

STZ–I mice demonstrated increased abundance of proteins involved in skeletal muscle oxidative stress compared

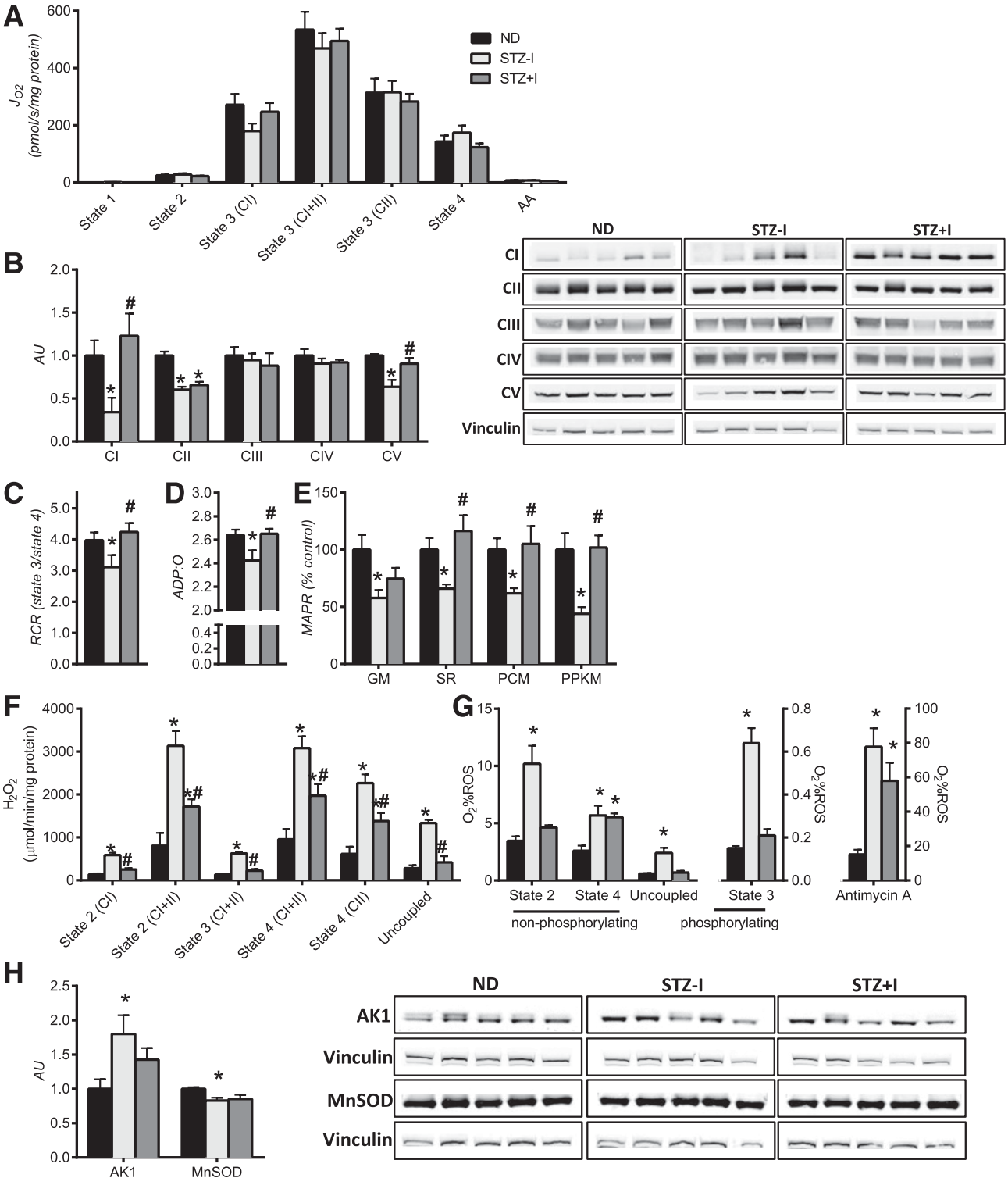

Figure 1—Insulin deprivation adversely affects skeletal muscle mitochondrial physiology. *A*: Oxygen consumption (JO_2) was not different across groups. Expression of mitochondrial respiratory CI and V proteins (*B*) and mitochondrial coupling efficiency, measured by respiratory control ratios (RCR) (*C*) and ADP:O ratio (*D*), was reduced by insulin deprivation and corrected by insulin treatment. *E*: Mitochondrial ATP production rate (MAPR) was significantly lower with insulin deprivation and restored with insulin therapy. *F*: Mitochondrial H_2O_2 emissions were elevated with insulin deprivation and partially reduced by insulin replacement across all respiratory states. *G*: O_2 consumption as a percent of ROS was higher in STZ–I. *H*: Increase in mitochondrial ROS production was associated with downregulation of mitochondrial MnSOD. Increased expression of AMP-sensitive adenylate kinase 1 (AK1) confirms the low-energy state of skeletal muscle in insulin-deprived animals. Substrate combinations description: GM, glutamate and malate; SR, succinate and rotenone; PCM, palmitoylcarnitine and malate; PPKM, palmitoylcarnitine, pyruvate, α-ketoglutarate, and malate. Data are means ± SEM (n = 13 per group for mitochondrial functional measurements, n = 6 for Western blot measurements). AA, amino acids; AU, arbitrary unit. *P < 0.05 vs. ND; #P < 0.05 vs. STZ–I group.

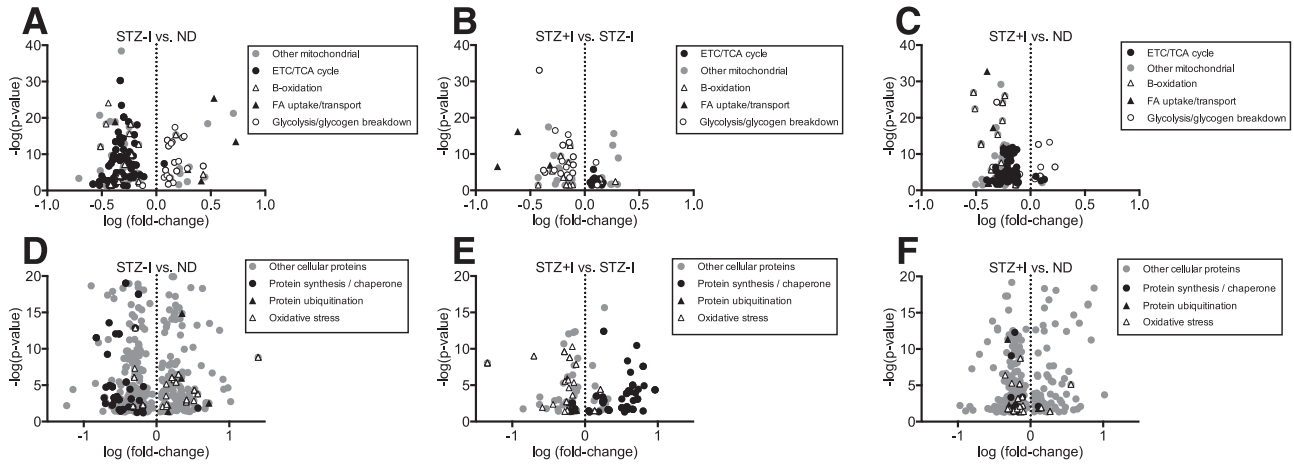

Figure 2—The effect of insulin deprivation and treatment on skeletal muscle proteome. *A*: Compared with ND, STZ–I exhibited reduced expression of mitochondrial proteins but increased proteins linked with FA uptake/transport and glycolysis/glycogen breakdown. These directional trends were reversed in STZ+I (*B*) but were still visible compared with ND (*C*). *D*: Protein markers of oxidative stress and ubiquitination were higher in STZ–I mice compared with ND, and proteins linked with protein synthesis were lower. These directional trends were reversed in STZ+I (*E*) to the levels comparable with ND mice (*F*). Only significantly affected proteins are shown on volcano plots ($-\log_{10} P > 1.301$). Individual protein names and expression values are given in Supplementary Table 2*A–F* for panels *A* to *F*, respectively.

with ND mice (Fig. 2*D* and Supplementary Table 2*D*). The expression of five nonmitochondrial antioxidant enzymes was significantly increased, whereas three mitochondria-targeted proteins were downregulated. A notable exception was observed for Parkinson protein 7 (PARK7/DJ-1), a redox-sensitive protein that regulates mitochondrial autophagy (mitophagy) (Supplementary Fig. 4). This observation suggests that insulin deprivation triggers a ROS-related compensatory mechanism at the level of mitochondria, which may increase mitophagy in STZ–I.

To address the above possibility, we focused on muscle proteins involved in the regulation of protein degradation and synthesis. Five ubiquitin-proteasome pathway proteins were significantly upregulated in STZ–I. Further, we used MS to measure the abundance of semitryptic peptides related to in vivo cellular protein degradation. Although the overall abundance of semitryptic peptides was similar in ND, STZ–I, and STZ+I groups, we observed significantly more peptides originating from mitochondrial proteins during insulin deprivation (Supplementary Fig. 5), indicating increased degradation of mitochondrial proteins.

The protein content of ribosomal proteins (18 subunits), three aminoacyl tRNA synthases, and four translation elongation factors (including mitochondrial TUFM) were significantly downregulated in the STZ–I group compared with the ND group (Fig. 2*D* and Supplementary Table 2*D*). Similar patterns were observed for four mitochondria-targeted and three cytosolic molecular chaperones. These proteomic changes suggest inhibition of protein synthesis in STZ–I animals, which was supported by decreased fractional synthesis rates of muscle proteins observed during insulin deprivation (Supplementary Fig. 6). The effects of insulin deprivation on proteins involved in protein ubiquitination and protein synthesis were reversed by insulin treatment in STZ+I mice (Fig. 2*E* and Supplementary Table 2*E*). The same was noted for mitochondrial PARK7/DJ-1 and mitochondrial semitryptic peptides content. Compared with ND mice, the STZ+I animals displayed similar expression of proteins involved in protein synthesis and degradation, with lower expression of those responsible for antioxidant defense (Fig. 2*F* and Supplementary Table 2*F*). These results provide proteomic evidence consistent with increased oxidative stress on proteins during insulin deprivation that is resolved with insulin treatment.

Pathway Enrichment Analysis

Pathway analysis was performed to provide additional insight into the major metabolic networks that were affected by insulin deprivation. Pathways involved in energy metabolism, oxidative damage, and protein synthesis were most affected in STZ–I (Fig. 3*A* and Supplementary Table 3*A*). Mitochondrial energy metabolism and muscle protein synthesis were downregulated in STZ–I, whereas glycolysis, glycogen degradation, and oxidative damage–related pathways were upregulated. Insulin treatment partially corrected metabolic alternations by mostly upregulating pathways responsible for oxidative phosphorylation and protein synthesis and substantially downregulating glycolysis-related and oxidative stress response pathways compared with STZ–I (Fig. 3*B* and Supplementary Table 3*B*). Of interest, pathways of fat oxidation and mitochondrial FA import (β-oxidation, L-carnitine shuttle) remained downregulated in STZ+I animals compared with ND. Compared with ND mice, the STZ+I animals displayed downregulation of mitochondrial metabolism and TCA cycle pathways and upregulation of glycolysis, albeit to a lesser degree than in STZ–I mice (Fig. 3*C* and

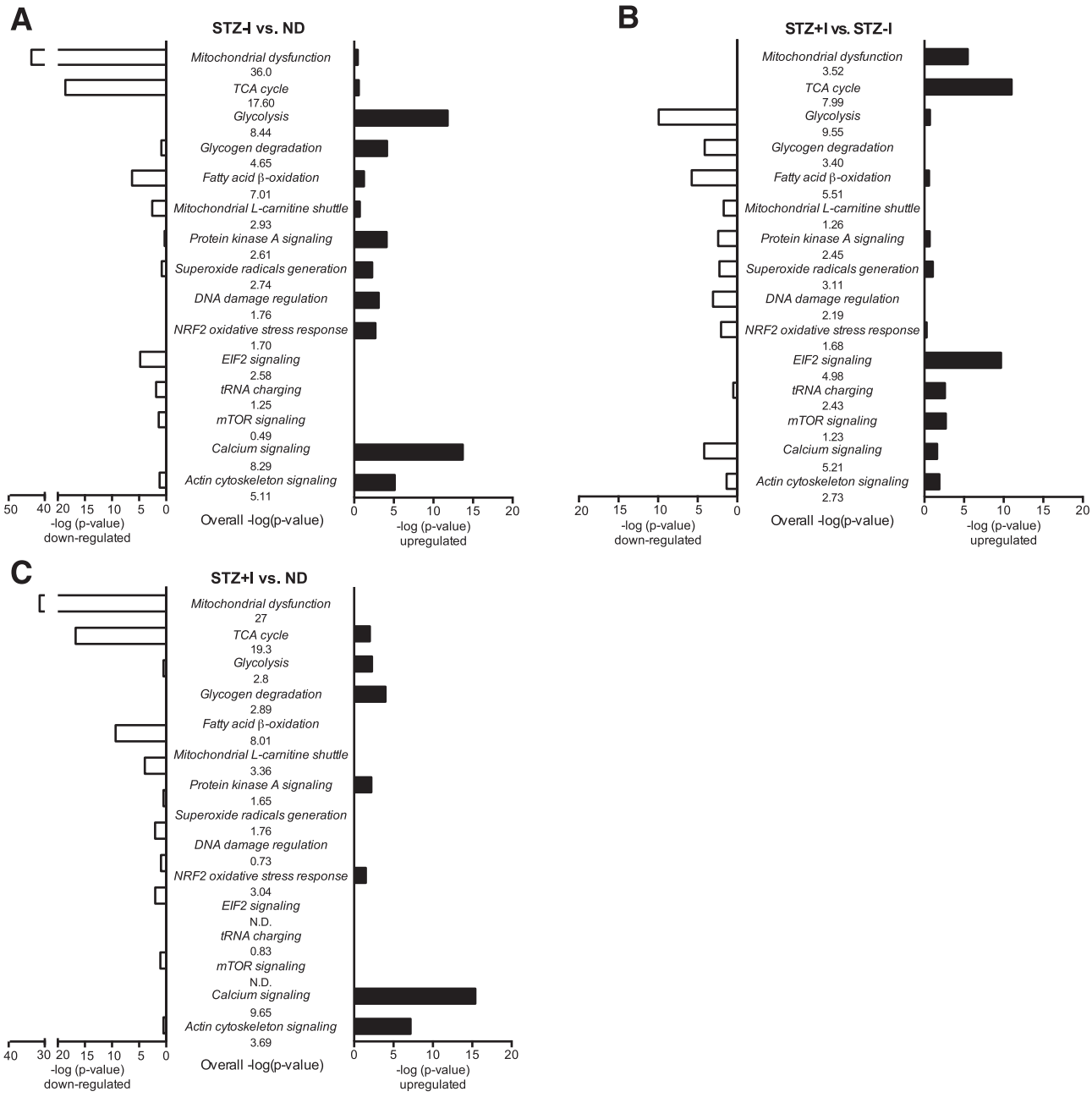

Figure 3—Canonical pathways affected by insulin deprivation and treatment. *A*: Pathways affected in STZ–I compared with ND animals. *B*: Pathways affected by insulin treatment (STZ+I) compared with diabetic insulin-deprived (STZ–I) mice. *C*: Pathways that distinguish between STZ+I and ND mice. The middle column of each graph lists the pathway name and the overall pathway score presented as $-\log_{10} P$ value. The □ bars display the pathway $-\log_{10} P$ value score calculated using only downregulated proteins, whereas ■ bars depict the same variable using only upregulated proteins. Significantly affected pathways display the $-\log_{10} P$ value score >1.3 ($P < 0.05$). All significantly affected pathways from STZ–I vs. ND, STZ+I vs. STZ–I, and STZ+I vs. ND comparisons are listed in Supplementary Table 3*A*, *B*, and *C*, respectively.

Supplementary Table 3*C*). Molecular pathways of protein synthesis, degradation, and oxidative damage were normalized in STZ+I animals compared with ND.

Products of Defective FA β-Oxidation Accumulate in Skeletal Muscle of STZ–I Animals

Figure 4*A* shows the expression profiles of 23 mitochondrial proteins that are involved in cellular FA uptake, mitochondrial FA uptake, acyl-carnitine efflux, and mitochondrial β-oxidation. To follow-up on the proteomic evidence of downregulation of muscle mitochondrial β-oxidation in the STZ–I group, we measured intramyocellular acyl-carnitines, which are biomarkers of inherited β-oxidation FA oxidation disorders (32). STZ–I mice accumulated short-chain (C2–C5) acyl-carnitines in skeletal muscle (Fig. 4*B* and *C*). Analysis of CPT1 and SCAD activity indices suggest inhibition of CPT1 and SCAD (Fig. 4*D*), which is in agreement with the proteomics and

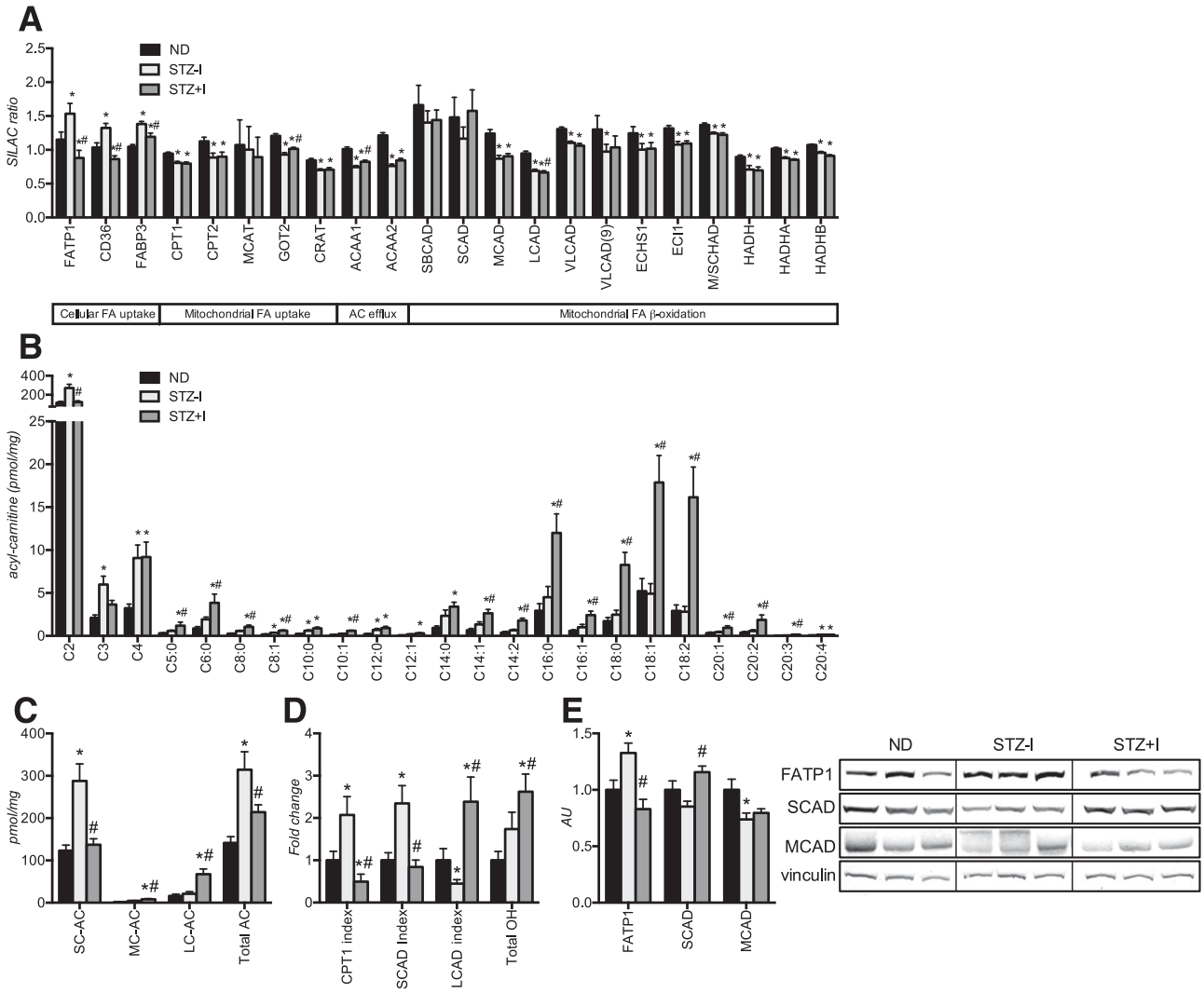

Figure 4—Both insulin deprivation and treatment leads to accumulation of acyl-carnitines and suggests incomplete fatty acid β-oxidation in skeletal muscle of T1D mice. Expression of FA intracellular transport and β-oxidation proteins is affected in insulin-deprived mice and not fully corrected by insulin replacement, as revealed by high-throughput proteomic analysis (*A*) and Western blot (*E*). Insulin deprivation increases skeletal muscle short-chain acyl-carnitine content (*B* and *C*) and elevates CPT1 and SCAD inhibition indexes (*D*). Insulin treatment corrects expression of proteins of intracellular FA uptake and short-chain FA β-oxidation (*A*) and reverses short-chain acyl-carnitine (SC-AC) accumulation and CPT1 and SCAD inhibition indexes (*B* and *C*) but leads to accumulation of medium-chain (MC-AC), long-chain (LC-AC), and 3-hydroxy (total OH) acyl-carnitine species (*B* and *C*) and increases the LCAD inhibition index (*D*). SC-AC, C2–C5 acyl-carnitines; MC-AC, C6–C12 acyl-carnitines; LC-AC, C14–C20 acyl-carnitines. Data are means ± SEM (n = 6 per group). AU, arbitrary unit; M/SCHAD, medium-/short-chain 3-hydroxyacyl-coenzyme A dehydrogenase. *P < 0.05 vs. ND; #P < 0.05 vs. STZ–I group.

Western blot results (Fig. 4*A* and *E*). Interestingly, insulin treatment normalized shortest-chain (C2 to C3) acyl-carnitine content, CPT1, and SCAD activity indices, yet significantly increased long-chain acyl-carnitine content and the long-chain acyl-CoA dehydrogenase (LCAD) index, suggesting inhibition of LCAD (Fig. 4*A* and *D*). Moreover, accumulation of 3-hydroxy acyl-carnitine molecular species (total OH, Fig. 4*D*) was evident in STZ+I. Together, these results provide evidence of insufficient FA oxidation in skeletal muscle in STZ–I, which could be explained on the basis of the paradoxical increase in FA transport proteins but decreased FA oxidative capacity.

Disruption of β-Oxidation in C2C12 Myotubes Under FA Load Leads to Mitochondrial Dysfunction

To determine whether disrupting β-oxidation under conditions of increased lipid load could trigger mitochondrial dysfunction in skeletal muscle cells, we measured mitochondrial oxygen consumption and ROS content of palmitate-treated C2C12 myotubes under β-oxidation inhibition. Because STZ–I mice exhibit metabolomic and proteomic signs of SCAD deficiency, we treated cells with MCPA, an inhibitor of SCAD and MCAD (33), and exposed cells to increased levels of palmitate. Treatment with MCPA suppressed respiration and coupling efficiency in the presence of palmitate but not in the

absence of palmitate (Fig. 5*A* and *B*). Inhibition of β-oxidation under lipid load led to significantly higher cellular ROS compared with control and palmitate-treated myotubes, which was visible only in the presence of palmitate and MCPA (Fig. 5*C*). The results indicate that mitochondrial capacity and coupling are reduced and that ROS production is increased when β-oxidation is inhibited under conditions of high FA availability, thus recapitulating the mitochondrial phenotype of the insulin-deprived diabetic mice.

DISCUSSION

The current study demonstrates the pivotal role of insulin in regulating mitochondrial physiology. During insulin deprivation, the mitochondrial uncoupling and decreased phosphorylation efficiency occurred in combination with elevated mitochondrial ROS production. We demonstrate that these mitochondrial derangements induced by insulin deficiency are accompanied by an imbalance between muscle lipid availability and oxidation, which is likely the source of excessive oxygen free radical emission. Insulin deprivation increases mobilization of FAs, and we observed upregulation of proteins involved in intracellular FA uptake, transport, and acyl-CoA conversion yet downregulated proteins that are responsible for FA storage and de novo synthesis. Despite this apparent shift toward lipid utilization during insulin deprivation, proteins involved in mitochondrial FA–CoA import and β-oxidation were downregulated, demonstrating a mismatch between FA uptake and β-oxidative capacity. This mismatch offers a mechanistic explanation for accumulation of intramyocellular lipid metabolites and ceramides in STZ–I animals (13,34).

The current study demonstrates that oxidative stress is elevated under conditions where lipid availability is high and β-oxidation capacity is decreased. Precedent literature links the oversupply of lipids with mitochondrial ROS production in muscle cell culture (35), rodent muscle (36), and in humans (37). Studies also suggest that plasma acyl-carnitine accumulation in T1D and T2D results from incomplete β-oxidation (17,18). The current study offers a mechanistic link between these two phenomena. The proteome measurements in the current study demonstrate that insulin deprivation decreased the abundance of β-oxidation proteins and increased markers of CPT1 and SCAD inhibition, causing incomplete lipid oxidation in the form of short-chain acyl carnitines. Moreover, inhibition of β-oxidation in muscle cells induced ROS production and decreased mitochondrial function in the presence of increased lipid availability. These results indicate that mitochondrial ROS emission arises from increased FA abundance in combination with a defective β-oxidation, leading to accumulation of incomplete FA oxidation products. In addition, despite increased expression of proteins involved in glycolysis and glycogenolysis, elevated PDHK4 suggests inhibition of PDH complex and decreased entry of glucose-derived pyruvate into the TCA cycle (34).

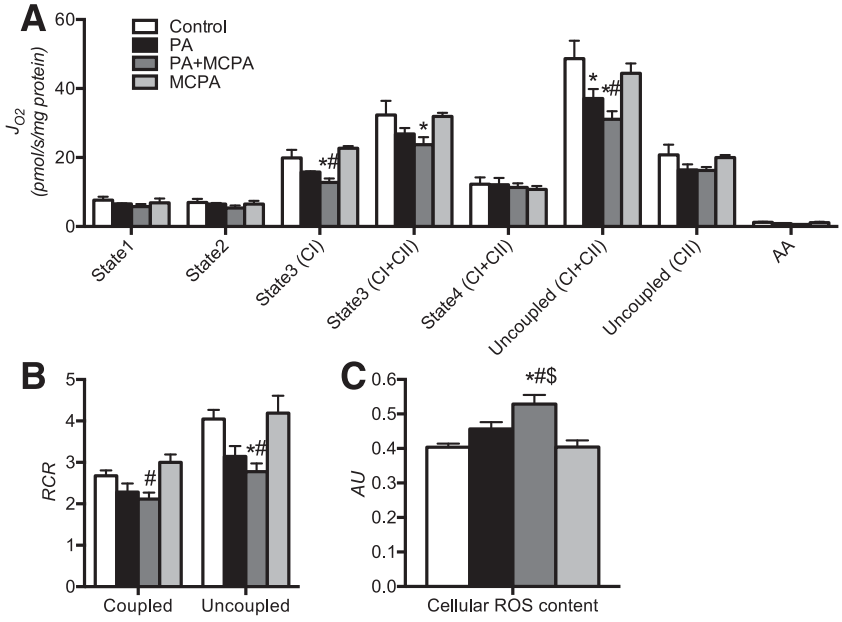

Figure 5—Inhibition of β-oxidation in palmitate-treated C2C12 cells mimics mitochondrial disturbances observed in skeletal muscle of diabetic animals. Inhibition of β-oxidation by MCPA (SCAD and MCAD inhibitor) significantly decreases mitochondrial O_2 consumption (JO_2) (*A*) and mitochondrial coupling efficiency (respiratory control ratio [RCR]) (*B*) and elevates cellular ROS content (*C*) in C2C12 cells treated with palmitate. The adverse effects of β-oxidation inhibition were observed only under both palmitate and MCPA treatment (PA+MCPA) and were not observed in control cells treated with MCPA. PA, palmitate-treated cells; PA+MCPA, palmitate- and MCPA-treated cells; MCPA, control cells treated with MCPA. Data are means ± SEM ($n = 3$ per experiment). AA, amino acids; AU, arbitrary unit. *$P < 0.05$ vs. control; #$P < 0.05$ vs. MCPA group; \$$P < 0.05$ vs. PA group.

Excess FA during insulin deprivation is expected to increase FA oxidation. FAs are natural ligands of skeletal muscle's peroxisome proliferator–activated receptor-α (PPARα) nuclear receptors, which regulate transcription of β-oxidation proteins. Surprisingly, we observed downregulation of PPARα-regulated proteins in muscle of STZ–I mice despite FA overload. Similar findings were shown in C2C12 myotubes treated with the CPT1 inhibitor etomoxir, where moderate suppression of FA oxidation triggered upregulation of PPARα signaling, whereas increasing inhibition led to profound downregulation of PPARα target genes (38). The inhibitory effect on PPARα signaling was dependent on increased oxidative stress, because antioxidants normalized PPARα signaling despite etomoxir treatment. In the current study, insulin deprivation triggered oxidative stress, which was accompanied by downregulation of most of the PPARα-dependent proteins, a finding consistent with decreased PPARα mRNA in STZ mice (39).

The effect of high ROS emission in STZ–I skeletal muscle is evident in the form of superoxide generation, DNA damage, increased protein degradation, and NRF2-mediated oxidative stress response. Reduced ROS-related damage to muscle proteins was found to be responsible for improved mitochondrial function in calorie-restricted older mice (22). Moreover, ROS-induced damage has been reported to cause decreased ATP production, which was ameliorated by stimulating mitochondrial DNA repair through mitochondria-targeted human OGG1 (35) or catalase (40) overexpression. These studies are consistent with our contention that decreased mitochondrial ATP production and coupling efficiency during insulin-deprivation results from increased mitochondrial ROS production consequent to imbalance between cellular FA uptake and oxidation. Indeed, insulin treatment of STZ mice increased mitochondrial coupling and phosphorylation efficiency, decreased oxidative stress, normalized plasma FFA and skeletal muscle lipid parameters (13), decreased short-chain FA β-oxidation products, and shifted whole-body metabolism toward carbohydrate utilization, as indicated by the higher respiratory quotient.

The reduction in mitochondrial efficiency during insulin deprivation is compounded by decreased abundance of mitochondrial proteins. Proteomic analysis of the current study revealed that most of the 51 subunits of mitochondrial respiratory complexes, as well as other molecules involved in ATP metabolism, such as adenine nucleotide translocases, mitochondrial solute carrier proteins, and many proteins localized to mitochondria, are diminished. Previous reports indicated that STZ-induced hypoinsulinemic mice show decreased expression of five subunits of respiratory complexes (41). The current study offers substantial support to the concept that insulin is a key regulator of mitochondrial biology (1). Specifically, insulin stimulated mitochondrial protein synthesis and mRNA expression in skeletal muscle of human and swine (2), increased mitochondrial oxidative capacity (1), and inhibited muscle protein degradation (9,42). Conversely, short-term insulin deprivation in individuals with T1D decreases mRNA expression of several mitochondrial proteins in skeletal muscle (5), highlighting an important role for insulin in regulating mitochondrial biogenesis. Here we advanced these findings by demonstrating that molecular pathways responsible for mitochondrial (TUFM) and cellular (EIF2) regulation of protein synthesis are significantly downregulated in the absence of insulin, which is confirmed by decreased skeletal muscle protein synthesis rates.

The proteomic survey also revealed that insulin deprivation activated the ubiquitin/proteasome pathway of protein degradation, which is responsible for removal of misfolded or damaged proteins (43). These results are consistent with the substantial increase in muscle protein degradation reported based on isotope-based studies in insulin-deprived individuals with T1D (8). In addition, we observed the downregulation of all major classes of chaperones and also increased abundance of semitryptic peptides originating from mitochondrial proteins in STZ–I, supporting a notion that a selective degradation of mitochondrial proteins occurs in the insulin-deprived state, which was corrected by insulin treatment.

A likely cause of this phenomenon is mitophagy due to mitochondrial oxidative damage, as recently observed in HeLa cells (44). Recent studies indicate that the PARK7/DJ-1 protein can stimulate mitophagy and mitochondrial recycling in neuronal cells under excessive mitochondrial oxidative damage (45,46). The current results indicate an accelerated mitochondrial protein degradation in skeletal muscle of STZ–I as increased ROS emission by muscle mitochondria is accompanied by decreased mitochondrial MnSOD expression, upregulation of PARK7/DJ-1, and elevation of semitryptic peptides of mitochondrial origin. Increased oxidative damage of mitochondrial proteins has led to defective β-oxidation due to inactivation of CPT1 protein by oxidative carbonylation (47). Therefore, reduced protein synthesis and increased autophagy are both likely responsible for the decrease in the content of mitochondrial proteins, leading to defective β-oxidation in STZ–I mice.

To our best knowledge this is the first study that links skeletal muscle mitochondrial energetic-to-proteome imbalance–based large-sale protein expression profile in diabetes. The purely proteomic study by Johnson et al. (48) in spontaneously diabetic BB-DP rats was able to identify only nine affected proteins, of which five were of blood plasma origin. Their study reported upregulation of ATP synthase and downregulation to enolase. We found some molecular similarities, with more numerous articles on proteome changes in T2D. The similar downregulation of PARK7/DJ-1 protein and increase in oxidative stress–related pathways was reported in myotubes derived from subjects with T2D, although accompanied by upregulation of mitochondrial, TCA, and ETC proteins, which is in clear opposition to our findings (49). The differences

are likely due to the treatment status and studying insulin-deficient versus insulin-deprived states. More similarities in skeletal muscle protein expression can be drawn between the current study and the results of Hwang et al. (50) regarding mitochondrial protein alternations and abundance of proteasomal proteins, albeit the latter study focused on T2D and obese individuals. Those data together indicate that although some molecular similarities exist between T1D and T2D skeletal muscle proteomes, the overall effect is significantly different, presumably due to the systemic insulin concentrations and tissue insulin resistance in T2D.

Insulin replacement did not completely restore the loss of mitochondrial protein abundance, β-oxidation enzymes, mitochondrial ROS emissions, or acyl-carnitine profile despite reversal of the diabetic phenotype, although protein synthesis and oxidative stress–related pathways returned to ND level. Interestingly, compared with controls, STZ+I animals had lower expression of FAs uptake and β-oxidation proteins, which shows that skeletal muscle lipid metabolism is still defective, even under insulin treatment. This suggests that some aspects of mitochondrial dysfunction can prevail in T1D when insulin therapy fails to fully restore HbA_{1c} levels to the same level as ND mice. Here, STZ mice that received exogenous insulin exhibited normalized plasma glucose in the fasted state, but postprandial glucose levels remained elevated, which frequently occurs in individuals with T1D (51). The same can be noted for plasma FFA content, which can show excessive postprandial elevation in patients with T1D compared with normal subjects (52). Postprandial FFA elevation additionally exacerbates hyperglycemia, possibly due to induction of fat-related insulin resistance (53–55). Many metabolic abnormalities are observed in diabetic dogs receiving insulin via systemic routes versus the portal route (31) that may also explain why not all proteomic/metabolic abnormalities are fully normalized by systemic insulin administration in STZ mice. Antioxidant treatment was shown to improve skeletal muscle mass, decrease protein ubiquitination and autophagy (56), reduce postprandial hyperglycemia and skeletal muscle oxidative stress mediators, enhance plasma antioxidant capacity (57), and, finally, improve mitochondrial function in STZ-induced diabetic mice (58).

The substantial body of current research underlines the importance of excessive lipid overabundance in the induction of metabolic derangements in all major body tissues. Although the current study shows that lipid-driven ROS production is the major contributor of mitochondrial dysfunction in skeletal muscle of STZ-induced diabetic mice, the other components of the T1D phenotype can affect mitochondrial physiology. Hyperketonemia is associated with increased vascular and immune cells ROS production (59) and also exerts mitoprotective effects in neuronal cells (60–62). Contrary to FAs, ketone bodies increase ROS in endothelial cells by unknown mechanism. Moreover, mitochondrial FA metabolism in T1D is hard to dissociate from ketones generation. Other factors, such as hyperglycemia, although associated with mitochondrial dysfunction, contrary to FAs, are unable to induce mitochondrial dysfunction in C2C12 myotubes (63). Finally, hypoinsulinemia and insulin resistance both associate with skeletal muscle mitochondrial dysfunction, suggesting that our findings are solely dependent on insulin action in skeletal muscle. Results by Sleigh et al. (64) and Kristensen et al. (65) showed that people with insulin receptor (INSR) mutation display mitochondrial dysfunction under normoglycemia, although involvement of intramuscular lipid accumulation was not ruled out in this study. In both studies, INSR mutants showed an increase in circulating FFA under basal or clamp conditions. Neither study excluded the possibility that increased FAs overabundance, intramuscular transport, and FA-driven ROS production are the major factors causing mitochondrial functional changes. Moreover, the observation by Kristensen et al. (65) that INSR mutants displayed a trend toward the decreased activity of β-HAD (β-hydroxy–acyl-CoA dehydrogenase, enzyme of β-oxidation pathway), noticeable only under lipid overload, supports our hypothesis that mismatch between FAs supply and oxidation drives ROS-related mitochondrial dysfunction in skeletal muscle.

Describing the rationale of the model that we have used is important. The model that has been extensively used in humans with T1D to study the effect of insulin deficiency involves transient withdrawal of insulin treatment (7,66,67). We used a similar approach in our STZ-induced diabetic mice treated with an insulin implant. These animals had no residual β-cell activity, and insulin withdrawal allowed us to observe the changes attributed solely to insulin deficiency, without interference of STZ toxicity, immediate insulinitis, hypoglycemia, and effects of stress, such as starvation, and inactivity caused by the T1D induction protocol. We treated all STZ-induced diabetic animals with insulin implants until normalization of body composition and glycemic control and then withdrew the insulin for a week. In contrast to other models of multiple low-dose STZ injections or spontaneously diabetic mice, such as NOD or Akita mice, BB rats display variable time of onset and degree of diabetes due to residual β-cell function (68,69). From a translational point of view, the model that we have used is the most appropriate in the study of the molecular effects of insulin deprivation and treatment.

In summary, the current study demonstrates that insulin deprivation in STZ-induced diabetic mice leads to a profound disturbance of energy metabolism and multilevel disruption of mitochondrial function in skeletal muscle. Specifically, insulin deprivation markedly reduced mitochondrial ATP synthesis, phosphorylation, and coupling efficiency and resulted in high ROS emission. These changes occur in association with increased expression of intramyocellular FA transport proteins despite decreased

expression of proteins involved in mitochondrial FA-CoA import and β-oxidation that may explain the marked accumulation of incomplete lipid oxidation products in skeletal muscle of insulin-deprived animals. The current results demonstrate that insulin deprivation alters the balance of proteins involved in FA transport and oxidation, leading to impaired mitochondrial function and increased oxidative stress in skeletal muscle.

Acknowledgments. The authors wish to express deep gratitude for the skillful technical work of Katherine Klaus, Dawn Morse, Jill Schimke, Daniel Jakaitis, and Bushra Ali (Division of Endocrinology, Diabetes, Metabolism, and Nutrition, Mayo Clinic College of Medicine, Rochester, MN).

Funding. Support for this work was provided by National Institutes of Health grants R01-DK-41973, Mayo Clinic Metabolomics Resource Core grant U24-DK-100469, Clinical and Translational Science Award grant UL1-TR-000135, Stephenson Fellowship (P.Z.), Indo-US Science and Technology Fellowship (2009), Indian Council of Medical Research International Fellowship (2013-14) (S.G.), and David H. Murdock-Dole Food Company Professorship (K.S.N.).

Duality of Interest. No potential conflicts of interest relevant to this article were reported.

Author Contributions. P.Z. and I.R.L. prepared the figures and drafted the manuscript. P.Z., I.R.L., and S.G. performed mitochondrial functional experiments. P.Z., I.R.L., S.G., H.R.B., S.D., and K.S.N. edited and revised the manuscript. P.Z., I.R.L., and S.D. analyzed data. P.Z., I.R.L., and K.S.N. interpreted results of experiments. P.Z. and S.G. performed animal experiments. P.Z., C.J.H.H., H.R.B., and S.D. performed SILAC-assisted proteomic analysis. P.Z. and K.S.N. conceived and designed the study. P.Z., I.R.L., S.G., C.J.H.H., H.R.B., S.D., and K.S.N. approved the final version of the manuscript. S.G. performed Western blotting analysis and cell culture experiments. K.S.N. coordinated and directed the project. K.S.N. is the guarantor of this work and, as such, had full access to all the data in the study and takes responsibility for the integrity of the data and the accuracy of the data analysis.

References

1. Stump CS, Short KR, Bigelow ML, Schimke JM, Nair KS. Effect of insulin on human skeletal muscle mitochondrial ATP production, protein synthesis, and mRNA transcripts. Proc Natl Acad Sci U S A 2003;100:7996–8001

2. Boirie Y, Short KR, Ahlman B, Charlton M, Nair KS. Tissue-specific regulation of mitochondrial and cytoplasmic protein synthesis rates by insulin. Diabetes 2001;50:2652–2658

3. Robinson MM, Soop M, Sohn TS, et al. High insulin combined with essential amino acids stimulates skeletal muscle mitochondrial protein synthesis while decreasing insulin sensitivity in healthy humans. J Clin Endocrinol Metab 2014; 99:E2574–E2583

4. Rizza RA, Jensen MD, Nair KS. Type 1 diabetes mellitus (insulin-dependent diabetes mellitus). In *Handbook of Physiology*. Jefferson LS, Cherrington AD, Goodman HM, Eds. Oxford University Press, 2001, p. 1093–1114

5. Karakelides H, Asmann YW, Bigelow ML, et al. Effect of insulin deprivation on muscle mitochondrial ATP production and gene transcript levels in type 1 diabetic subjects. Diabetes 2007;56:2683–2689

6. Charlton MR, Nair KS. Role of hyperglucagonemia in catabolism associated with type 1 diabetes: effects on leucine metabolism and the resting metabolic rate. Diabetes 1998;47:1748–1756

7. Nair KS, Garrow JS, Ford C, Mahler RF, Halliday D. Effect of poor diabetic control and obesity on whole body protein metabolism in man. Diabetologia 1983;25:400–403

8. Nair KS, Ford GC, Ekberg K, Fernqvist-Forbes E, Wahren J. Protein dynamics in whole body and in splanchnic and leg tissues in type I diabetic patients. J Clin Invest 1995;95:2926–2937

9. Chow LS, Albright RC, Bigelow ML, Toffolo G, Cobelli C, Nair KS. Mechanism of insulin's anabolic effect on muscle: measurements of muscle protein synthesis and breakdown using aminoacyl-tRNA and other surrogate measures. Am J Physiol Endocrinol Metab 2006;291:E729–E736

10. Barrett EJ, Schwartz RG, Francis CK, Zaret BL. Regulation by insulin of myocardial glucose and fatty acid metabolism in the conscious dog. J Clin Invest 1984;74:1073–1079

11. Jaleel A, Klaus KA, Morse DM, et al. Differential effects of insulin deprivation and systemic insulin treatment on plasma protein synthesis in type 1 diabetic people. Am J Physiol Endocrinol Metab 2009;297:E889–E897

12. Charlton MR, Balagopal P, Nair KS. Skeletal muscle myosin heavy chain synthesis in type 1 diabetes. Diabetes 1997;46:1336–1340

13. Zabielski P, Blachnio-Zabielska A, Lanza IR, et al. Impact of insulin deprivation and treatment on sphingolipid distribution in different muscle subcellular compartments of streptozotocin-diabetic C57Bl/6 mice. Am J Physiol Endocrinol Metab 2014;306:E529–E542

14. Seifert EL, Estey C, Xuan JY, Harper ME. Electron transport chain-dependent and -independent mechanisms of mitochondrial H2O2 emission during long-chain fatty acid oxidation. J Biol Chem 2010;285:5748–5758

15. Bene J, Márton M, Mohás M, et al. Similarities in serum acylcarnitine patterns in type 1 and type 2 diabetes mellitus and in metabolic syndrome. Ann Nutr Metab 2013;62:80–85

16. Jacobson J, Midyett LK, Garg U, Sherman AK, Patel C. Biochemical evidence for reduced carnitine palmitoyl transferase 1 (CPT-1) activity in type 1 diabetes mellitus. J Diabetes Metab 2011;2:144

17. Mihalik SJ, Goodpaster BH, Kelley DE, et al. Increased levels of plasma acylcarnitines in obesity and type 2 diabetes and identification of a marker of glucolipotoxicity. Obesity (Silver Spring) 2010;18:1695–1700

18. Adams SH, Hoppel CL, Lok KH, et al. Plasma acylcarnitine profiles suggest incomplete long-chain fatty acid beta-oxidation and altered tricarboxylic acid cycle activity in type 2 diabetic African-American women. J Nutr 2009;139:1073–1081

19. Bugger H, Chen D, Riehle C, et al. Tissue-specific remodeling of the mitochondrial proteome in type 1 diabetic akita mice. Diabetes 2009;58:1986–1997

20. Baseler WA, Dabkowski ER, Jagannathan R, et al. Reversal of mitochondrial proteomic loss in Type 1 diabetic heart with overexpression of phospholipid hydroperoxide glutathione peroxidase. Am J Physiol Regul Integr Comp Physiol 2013;304:R553–R565

21. Levine JA, Nygren J, Short KR, Nair KS. Effect of hyperthyroidism on spontaneous physical activity and energy expenditure in rats. J Appl Physiol (1985) 2003;94:165–170

22. Lanza IR, Zabielski P, Klaus KA, et al. Chronic caloric restriction preserves mitochondrial function in senescence without increasing mitochondrial biogenesis. Cell Metab 2012;16:777–788

23. Pagliarini DJ, Calvo SE, Chang B, et al. A mitochondrial protein compendium elucidates complex I disease biology. Cell 2008;134:112–123

24. Jaleel A, Short KR, Asmann YW, et al. In vivo measurement of synthesis rate of individual skeletal muscle mitochondrial proteins. Am J Physiol Endocrinol Metab 2008;295:E1255–E1268

25. Zabielski P, Ford GC, Persson XM, Jaleel A, Dewey JD, Nair KS. Comparison of different mass spectrometry techniques in the measurement of L-[ring-(13)C6] phenylalanine incorporation into mixed muscle proteins. J Mass Spectrom 2013; 48:269–275

26. Chace DH, DiPerna JC, Mitchell BL, Sgroi B, Hofman LF, Naylor EW. Electrospray tandem mass spectrometry for analysis of acylcarnitines in dried postmortem blood specimens collected at autopsy from infants with unexplained cause of death. Clin Chem 2001;47:1166–1182

27. Fingerhut R, Röschinger W, Muntau AC, et al. Hepatic carnitine palmitoyltransferase I deficiency: acylcarnitine profiles in blood spots are highly specific. Clin Chem 2001;47:1763–1768

28. Boyle KE, Zheng D, Anderson EJ, Neufer PD, Houmard JA. Mitochondrial lipid oxidation is impaired in cultured myotubes from obese humans. Int J Obes 2012;36:1025–1031

29. Vrablic AS, Albright CD, Craciunescu CN, Salganik RI, Zeisel SH. Altered mitochondrial function and overgeneration of reactive oxygen species precede the induction of apoptosis by 1-O-octadecyl-2-methyl-rac-glycero-3-phosphocholine in p53-defective hepatocytes. FASEB J 2001;15:1739–1744
30. Nair KS, Halliday D, Garrow JS. Increased energy expenditure in poorly controlled Type 1 (insulin-dependent) diabetic patients. Diabetologia 1984;27:13–16
31. Freyse EJ, Fischer U, Knospe S, Ford GC, Nair KS. Differences in protein and energy metabolism following portal versus systemic administration of insulin in diabetic dogs. Diabetologia 2006;49:543–551
32. de Sain-van der Velden MG, Diekman EF, Jans JJ, et al. Differences between acylcarnitine profiles in plasma and bloodspots. Mol Genet Metab 2013; 110:116–121
33. Wenz A, Thorpe C, Ghisla S. Inactivation of general acyl-CoA dehydrogenase from pig kidney by a metabolite of hypoglycin A. J Biol Chem 1981;256:9809–9812
34. Thankamony A, Tossavainen PH, Sleigh A, et al. Short-term administration of pegvisomant improves hepatic insulin sensitivity and reduces soleus muscle intramyocellular lipid content in young adults with type 1 diabetes. J Clin Endocrinol Metab 2014;99:639–647
35. Yuzefovych LV, Solodushko VA, Wilson GL, Rachek LI. Protection from palmitate-induced mitochondrial DNA damage prevents from mitochondrial oxidative stress, mitochondrial dysfunction, apoptosis, and impaired insulin signaling in rat L6 skeletal muscle cells. Endocrinology 2012;153:92–100
36. Lambertucci RH, Hirabara SM, Silveira LdosR, Levada-Pires AC, Curi R, Pithon-Curi TC. Palmitate increases superoxide production through mitochondrial electron transport chain and NADPH oxidase activity in skeletal muscle cells. J Cell Physiol 2008;216:796–804
37. Anderson EJ, Lustig ME, Boyle KE, et al. Mitochondrial H2O2 emission and cellular redox state link excess fat intake to insulin resistance in both rodents and humans. J Clin Invest 2009;119:573–581
38. Cabrero A, Alegret M, Sanchez RM, Adzet T, Laguna JC, Carrera MV. Increased reactive oxygen species production down-regulates peroxisome proliferator-activated alpha pathway in C2C12 skeletal muscle cells. J Biol Chem 2002;277: 10100–10107
39. Yechoor VK, Patti ME, Saccone R, Kahn CR. Coordinated patterns of gene expression for substrate and energy metabolism in skeletal muscle of diabetic mice. Proc Natl Acad Sci U S A 2002;99:10587–10592
40. Lee HY, Choi CS, Birkenfeld AL, et al. Targeted expression of catalase to mitochondria prevents age-associated reductions in mitochondrial function and insulin resistance. Cell Metab 2010;12:668–674
41. Franko A, von Kleist-Retzow JC, Böse M, et al. Complete failure of insulin-transmitted signaling, but not obesity-induced insulin resistance, impairs respiratory chain function in muscle. J Mol Med (Berl) 2012;90:1145–1160
42. Rennie MJ. Anabolic resistance: the effects of aging, sexual dimorphism, and immobilization on human muscle protein turnover. Appl Physiol Nutr Metab 2009;34:377–381
43. Shang F, Taylor A. Ubiquitin-proteasome pathway and cellular responses to oxidative stress. Free Radic Biol Med 2011;51:5–16
44. Wang Y, Nartiss Y, Steipe B, McQuibban GA, Kim PK. ROS-induced mitochondrial depolarization initiates PARK2/PARKIN-dependent mitochondrial degradation by autophagy. Autophagy 2012;8:1462–1476
45. Joselin AP, Hewitt SJ, Callaghan SM, et al. ROS-dependent regulation of Parkin and DJ-1 localization during oxidative stress in neurons. Hum Mol Genet 2012;21:4888–4903
46. Krebiehl G, Ruckerbauer S, Burbulla LF, et al. Reduced basal autophagy and impaired mitochondrial dynamics due to loss of Parkinson's disease-associated protein DJ-1. PLoS One 2010;5:e9367
47. Serviddio G, Giudetti AM, Bellanti F, et al. Oxidation of hepatic carnitine palmitoyl transferase-I (CPT-I) impairs fatty acid beta-oxidation in rats fed a methionine-choline deficient diet. PLoS One 2011;6:e24084
48. Johnson DT, Harris RA, French S, Aponte A, Balaban RS. Proteomic changes associated with diabetes in the BB-DP rat. Am J Physiol Endocrinol Metab 2009; 296:E422–E432
49. Al-Khalili L, de Castro Barbosa T, Ostling J, et al. Profiling of human myotubes reveals an intrinsic proteomic signature associated with type 2 diabetes. Adv Integr Med 2014;2:25–38
50. Hwang H, Bowen BP, Lefort N, et al. Proteomics analysis of human skeletal muscle reveals novel abnormalities in obesity and type 2 diabetes. Diabetes 2010;59:33–42
51. Russell SJ, El-Khatib FH, Sinha M, et al. Outpatient glycemic control with a bionic pancreas in type 1 diabetes. N Engl J Med 2014;371:313–325
52. Van Waarde WM, Odink RJ, Rouwé C, et al. Postprandial chylomicron clearance rate in late teenagers with diabetes mellitus type 1. Pediatr Res 2001; 50:611–617
53. Wolpert HA, Atakov-Castillo A, Smith SA, Steil GM. Dietary fat acutely increases glucose concentrations and insulin requirements in patients with type 1 diabetes: implications for carbohydrate-based bolus dose calculation and intensive diabetes management. Diabetes Care 2013;36:810–816
54. Smart CE, Evans M, O'Connell SM, et al. Both dietary protein and fat increase postprandial glucose excursions in children with type 1 diabetes, and the effect is additive. Diabetes Care 2013;36:3897–3902
55. Wolever TM, Mullan YM. Sugars and fat have different effects on postprandial glucose responses in normal and type 1 diabetic subjects. Nutr Metab Cardiovasc Dis 2011;21:719–725
56. Ono T, Takada S, Kinugawa S, Tsutsui H. Curcumin ameliorates skeletal muscle atrophy in type 1 diabetic mice by inhibiting protein ubiquitination. Exp Physiol 2015;100:1052–1063
57. Ndisang JF, Jadhav A. Heme oxygenase system enhances insulin sensitivity and glucose metabolism in streptozotocin-induced diabetes. Am J Physiol Endocrinol Metab 2009;296:E829–E841
58. Bravard A, Bonnard C, Durand A, et al. Inhibition of xanthine oxidase reduces hyperglycemia-induced oxidative stress and improves mitochondrial alterations in skeletal muscle of diabetic mice. Am J Physiol Endocrinol Metab 2011;300:E581–E591
59. Jain SK, McVie R, Bocchini JA Jr. Hyperketonemia (ketosis), oxidative stress and type 1 diabetes. Pathophysiology 2006;13:163–170
60. Maalouf M, Sullivan PG, Davis L, Kim DY, Rho JM. Ketones inhibit mitochondrial production of reactive oxygen species production following glutamate excitotoxicity by increasing NADH oxidation. Neuroscience 2007;145:256–264
61. Kim Y, Vallejo J, Rho JM. Ketones prevent synaptic dysfunction induced by mitochondrial respiratory complex inhibitors. J Neurochem 2010;114:130–141
62. Milder J, Patel M. Modulation of oxidative stress and mitochondrial function by the ketogenic diet. Epilepsy Res 2012;100:295–303
63. Jheng HF, Tsai PJ, Guo SM, et al. Mitochondrial fission contributes to mitochondrial dysfunction and insulin resistance in skeletal muscle. Mol Cell Biol 2012;32:309–319
64. Sleigh A, Raymond-Barker P, Thackray K, et al. Mitochondrial dysfunction in patients with primary congenital insulin resistance. J Clin Invest 2011;121: 2457–2461
65. Kristensen JM, Skov V, Petersson SJ, et al. A PGC-1α- and muscle fibre type-related decrease in markers of mitochondrial oxidative metabolism in skeletal muscle of humans with inherited insulin resistance. Diabetologia 2014; 57:1006–1015
66. Katz H, Homan M, Velosa J, Robertson P, Rizza R. Effects of pancreas transplantation on postprandial glucose metabolism. N Engl J Med 1991;325: 1278–1283
67. Tessari P, Nosadini R, Trevisan R, et al. Defective suppression by insulin of leucine-carbon appearance and oxidationin type 1, insulin-dependent diabetes mellitus. Evidence for insulin resistance involving glucose and amino acid metabolism. J Clin Invest 1986;77:1797–1804
68. Chatzigeorgiou A, Halapas A, Kalafatakis K, Kamper E. The use of animal models in the study of diabetes mellitus. In Vivo 2009;23:245–258
69. Graham ML, Schuurman HJ. Validity of animal models of type 1 diabetes, and strategies to enhance their utility in translational research. Eur J Pharmacol 2015;759:221–230